European Journal of Pharmaceutical Sciences 128 (2019) 18–26

Contents lists available at ScienceDirect

European Journal of Pharmaceutical Sciences

journal homepage: www.elsevier.com/locate/ejps

Development of a joint population pharmacokinetic model of ezetimibe and its conjugated metabolite

Soulele K.[a], Karalis V.[a,b,*]

[a] Department of Pharmacy, School of Health Sciences, National and Kapodistrian University of Athens, 15784 Athens, Greece
[b] Institute of Applied and Computational Mathematics (IACM), Foundation of Research and Technology Hellas (FORTH), Greece

ARTICLE INFO

Keywords:
Enterohepatic recirculation
Joint population pharmacokinetic model
Ezetimibe
Ezetimibe glucuronide

ABSTRACT

Ezetimibe (EZE) is an extensively used antihyperlipidemic drug with an important cholesterol lowering activity. It undergoes extensive first-pass metabolism to form its active glucuronide metabolite (EZEG). Both drugs exhibit complex pharmacokinetic profiles attributed mainly to repetitive enterohepatic kinetics. The aim of the present study was the investigation of EZE and EZEG pharmacokinetics (PK), through the development of a joint population pharmacokinetic model able to characterize their kinetic processes and enterohepatic recirculation simultaneously. Concentration-time data derived from a bioequivalence study in 28 healthy subjects were used for the analysis. Population PK modeling was performed on the obtained data using nonlinear mixed effect modeling approach, where different methodologies were applied for the description of the complex metabolism and recirculation processes of the two compounds. EZE and EZEG concentrations were best described by a population PK model incorporating first-pass metabolism and an enterohepatic recirculation loop, accounting for the recycling process of the two moieties. This is the first joint population pharmacokinetic model describing the kinetics of both EZE and EZEG.

1. Introduction

Elevated serum cholesterol is a well-known risk factor for the development of coronary heart disease. Hypercholesterolemia has been strongly associated with heart disease mortality through various animal and clinical observations, which is further confirmed by epidemiological studies showing a strong relationship between serum total cholesterol and certain cardiovascular diseases (Hajar, 2017; Klag et al., 1993). Elevated serum cholesterol levels may occur through multiple processes, and apart from the de novo cholesterol synthesis, intestinal absorption of exogenous (dietary) and endogenous (biliary) cholesterol, may further lead to a less favorable lipid and atherogenic profile (Sweeney and Johnson, 2007).

Ezetimibe (EZE) is one of the first representatives of lipid-lowering drugs which act via inhibition of the absorption of exogenous and endogenous cholesterol, resulting in the reduction of intracellular cholesterol (Sweeney and Johnson, 2007). EZE has been shown to have a local action at the brush border of the small intestine, where it effectively blocks the uptake of cholesterol by enterocytes, while the absorption of triglycerides, fat-soluble vitamins or bile acids remains unaffected (Sweeney and Johnson, 2007; van Heek and Davis, 2002). This leads to inhibition of cholesterol systemic absorption which is finally excreted in the feces (Florentin et al., 2008; van Heek and Davis, 2002).

Following oral administration, ezetimibe is readily absorbed and rapidly metabolized to a great extent in the intestine, via glucuronidation of the 4-hydroxy phenyl group, with approximately 90% of the total drug in plasma being in the form of the equally potent

Abbreviations: BE, bioequivalence; BSV%, percent between subject variability; EHC, enterohepatic recirculation; EZE, ezetimibe; EZEG, ezetimibe glucuronide; F, fraction of bioavailable dose; GB, gallbladder; GI, gastrointestinal tract; kam, first-order absorption rate constant of EZEG; kap, first-order absorption rate constant of EZE; kelm, first-order elimination rate constant of EZEG; kelp, first-order elimination rate constant of EZE; kg1 & kg2, first-order constants for bile release into the EZE and EZEG central compartments, respectively; kmb, first-order transfer rate of EZEG from its central compartment to gallbladder compartment; kpm, first-order formation rate constant of EZEG; PK, pharmacokinetic; Qm/F, apparent inter-compartmental clearance of EZEG; Qp/F, apparent inter-compartmental clearance of EZE; R, reference product; RSE%, percent relative standard error; T, test product; Vcp/F, apparent volume of drug distribution of the central compartment for EZE; Vcm/F, apparent volume of drug distribution of the central compartment for EZEG; Vpm/F, apparent volume of drug distribution of the peripheral compartment for EZEG; Vpp/F, apparent volume of drug distribution of the peripheral compartment for EZE

* Corresponding author at: Laboratory of Biopharmaceutics - Pharmacokinetics, Department of Pharmacy, School of Health Sciences, National and Kapodistrian University of Athens, Athens 15784, Greece.
E-mail address: vkaralis@pharm.uoa.gr (V. Karalis).

https://doi.org/10.1016/j.ejps.2018.11.018
Received 12 September 2018; Received in revised form 18 November 2018; Accepted 18 November 2018
Available online 19 November 2018
0928-0987/

ezetimibe-glucuronide metabolite (EZEG) (Ezzet et al., 2001a; Ghosal et al., 2004; Kosoglou et al., 2005; Lipka, 2003). Ezetimibe undergoes first-pass metabolism in the intestine and liver to its glucuronide conjugate (Jeu and Cheng, 2003; Patrick et al., 2002; van Heek and Davis, 2002), both moieties reaching maximal concentrations in the plasma within 2 to 3 h (Lipka, 2003). Once glucuronidated, EZEG is excreted through the gallbladder back in the intestinal lumen, such that EZE is delivered back to its site of action through hydrolysis of the conjugate by β-glucuronidase (van Heek and Davis, 2002).

Both EZE and EZEG show multiple peaks in their concentration-time profiles suggestive of an extensive enterohepatic recirculation (EHC) (de Waart et al., 2009; Kosoglou et al., 2005). It is noted that this recirculation process ensures the repeated delivery of the moieties back to the intestine, where it can be re-absorbed and exert its pharmacologic effects. This leads to a prolonged cholesterol lowering activity and a limited peripheral exposure, contributing to the favorable efficacy and safety profile of the drug (Lipka, 2003; van Heek and Davis, 2002).

Due to the great influence of the first-pass metabolism and enterohepatic recirculation process on the therapeutic profile of ezetimibe, knowledge of its pharmacokinetic (PK) properties is of crucial importance. In this respect, many PK analyses have been performed for ezetimibe so far, applied mainly to the total EZE concentrations, defined as the sum of unconjugated ezetimibe and ezetimibe-glucuronide (Ezzet et al., 2001b; Kosoglou et al., 2004, 2005). In the same vein, two population pharmacokinetic models have been also developed, describing again the systemic course of total ezetimibe concentrations (Ezzet et al., 2001b; Soulele and Karalis, 2018). However, since both EZE and EZEG are found to be pharmacologically active and undergo an extensive systemic recycling, a simultaneous analysis of these two moieties can provide further insight into their pharmacokinetic properties and more adequately characterize their interrelated metabolism and elimination processes.

Therefore, the aim of the present analysis was to investigate the pharmacokinetics of both EZE and EZEG simultaneously, using population pharmacokinetic modeling approaches. In this vein, we aimed to develop a joint population PK model for the description of the absorption and the complex distribution properties of ezetimibe and its active glucuronide metabolite. In order to accomplish this task, a series of structural models were developed and compared for their performance based on their predictive ability and the adequate characterization of the underlying physiological processes.

2. Materials and methods

2.1. Subjects and study design

The concentration-time data used in this analysis came from an open-label, single-dose, randomized 2 × 2 crossover bioequivalence (BE) study, in healthy adult volunteers comparing a single-dose of Ezetimibe 10 mg Tablets (Rafarm S.A. Athens, Greece) or Ezetrol® 10 mg Tablets (Merck Sharp & Dohme S.A.), under fasting conditions. The study was performed according to the Good Clinical Practice guidelines issued by the International Conference on Harmonization and followed the principles of the Declaration of Helsinki. The National (Anveshhan) Independent Ethics Committee reviewed and approved the study protocol, while a written informed consent was obtained from each subject prior to enrolment in the study.

In total 36 subjects were initially enrolled in the BE study. All subjects underwent the required physical and biochemical examinations, and a thorough medical history was obtained by each participant to ensure their health status. Subjects were excluded in case of history, or presence, of significant disease (cardiovascular or other), concomitant therapy affecting liver function or any other prescribed medication during the last 30 days, intolerance or hypersensitivity to the active substance or any of the formulation excipients, presence or history of alcohol/drug abuse, smoking, urticaria or any other significant allergic reaction. Subjects were also omitted from the study, if they had donated over 450 mL of blood during 3 months before the initiation of the study, in cases of significant blood loss or other major illness, or if they showed positive tests in HIV or hepatitis B/C tests.

In each study period, subjects were fasted overnight for at least 10 h with access to water only. On treatment days, study participants received a single dose of 10 mg ezetimibe administered as an oral test Ezetimibe 10 mg tablet (Rafarm S.A. Athens, Greece) or the reference Ezetrol® 10 mg tablet (Merck Sharp & Dohme S.A.), with 240 mL of water. Standardized meals were then provided at 4, 8, 12, and 24 h after drug administration. In total, 26 blood samples (6.0 mL) were obtained from each participant, starting before drug administration and at 0.33, 0.67, 1, 1.33, 1.67, 2, 2.5, 3, 4, 4.5, 5, 5.5, 6, 6.5, 7, 8, 10, 12, 14, 16, 24, 36, 48, 72, and 96 h post-dose. All blood samples were centrifuged immediately after collection and stored frozen at −80 °C until analysis. After a two-week washout, subjects received the alternate formulation during the second study period and the same procedures were followed. EZE and EZEG were quantified in the collected samples using a validated liquid chromatography/tandem mass spectrometry (HPLC-MS/MS) method. Details describing the analytical assay are provided in our previous study (Soulele and Karalis, 2018).

2.2. Non-compartmental pharmacokinetic analysis

Ezetimibe (both EZE and EZEG) C-t data were analyzed using non-compartmental analysis which led to the estimation of the following PK parameters: the maximum observed plasma concentration (Cmax), the area under the C-t curve up to the last measured concentration (AUCt), and the area under the C-t curve extrapolated to infinity (AUCinf). Estimation of the two AUC areas was made by applying the linear trapezoidal rule. The entire analysis was made in WinNonlin® v.5.0.1 (Pharsight).

2.3. Population pharmacokinetic analysis

For the purposes of this analysis, ezetimibe dose as well as plasma EZE and EZEG concentrations were converted into their molar equivalents (nmol/L) by dividing with their molecular weight (EZE: 409.4 g/mol; EZEG: 585.5 g/mol). The data of both drugs were analyzed in Monolix® (version 2016R1, Lixoft). The SAEM (i.e., Stochastic Approximation Expectation Maximization) algorithm was used with the following settings; the maximal numbers of stochastic (k1) and cooling (k2) iterations were fixed at 500 and 200, respectively, using the automatic stopping rules and one Markov chain. Data below the limit of quantification were considered as 'missing' and were omitted from the analysis, while the option for treating them as 'cens' values was also tested. Besides, since the majority (over 95%) of the concentration values at the 96 h time-point was below the lower limit of quantitation, the dataset was further truncated at the nearest earlier time point i.e., at 72 h. Moreover, since the obtained data derived from a crossover BE study, the C-t data of the two compounds obtained from the different drug products (test and reference) and the two treatment periods were combined setting "treatment" and "period" effects as potential covariates in the final dataset. Following data treatment, 1501 and 1490 data points for EZE and EZEG, respectively, were available for the population PK analysis.

Population pharmacokinetic modeling was performed simultaneously both for EZE and EZEG. Since both undergo enterohepatic recirculation, this attribute was incorporated in the developed models by presuming a hypothetical gallbladder compartment accounting for the re-distribution process. All these models were written in the form of ordinary differential equations in the MLXTRAN language of Monolix®.

In this context, different PK models were developed, like one-, two-, and three-compartment distribution models, for EZE and EZEG. In conjunction with models encompassing aspects like first-pass metabolism in the gastrointestinal (GI) tract, we also tested the presence of

hypothetical gallbladder compartments (one or two), different bile release kinetics (first-order or bolus), variant times and durations of gallbladder emptying, consideration of both renal and fecal elimination, etc. In addition, the existence of a dose apportionment parameter for first-pass metabolism or accordingly a parameter accounting for the fraction of drug undergoing enterohepatic recirculation were evaluated for potential improvements in the final model.

In principle, in most PK models, following oral administration the drug is presented in the gastrointestinal compartment, where a fraction (F) of dose enters the EZE central compartment and the remaining fraction (1-F) goes to the EZEG central compartment. Thereafter, the two moieties are transferred into their peripheral compartments, undergo enterohepatic recirculation or are permanently eliminated from the system.

For the purposes of this study, all PK models were parameterized in terms of micro-constants where the symbols 'm' and 'p', next to each PK parameter, refer to EZEG and EZE, respectively. The choice of using micro-constants allowed us to examine several different linkages among the compartments. Indeed, absorption kinetics was expressed in the form of absorption rate constants (kap, kam), apparent volumes of distribution for the central (Vcp, Vcm) and peripheral (Vpp, Vpm) compartments, intercompartmental clearances (Qp, Qm) and elimination rate constants (kelp, kelm). Since bioavailability fraction (F) could not be quantified, volumes of distribution and intercompartmental clearances reflected their apparent values namely, Vcp/F, Vpm/F, Qp/F etc. For the EHC component of the model, the additional parameters tested for their performance, were the first-order constants for re-distribution of drugs (kpm, kpb), the gallbladder release rate constants (kg1 and kg2), the fraction of drug following EHC, and the fecal elimination rate constant. Gallbladder first-order release rate constants were either allowed to be freely estimated, or fixed to a relatively high value (e.g., $20\,h^{-1}$) in order to mimic the bolus impulse of gallbladder emptying. Bile release was further controlled by different switch functions to account for the intermittent nature of the gallbladder emptying process. Different hypotheses were tested in respect to the time and duration of gallbladder emptying. These scenarios were based on the study protocol information regarding the standardized meal intake (at 4, 8, 12, and 24 h post-dose), the obtained C-t profile, and physiological considerations regarding gallbladder function.

Most PK model parameters followed log-normal distribution, whereas logit-transformation was also used for certain parameters assumed to be constrained on the 0–1 scale (e.g. fraction of drug following EHC, fraction of drug undergoing first-pass metabolism). The stochastic model accounted for the between-subject, inter-occasion, and residual unexplained variability, while the covariate model described the potential correlations between certain covariates and model PK parameters. Different residual error models were evaluated in this respect, consisting of additive, proportional, exponential and combined (additive & proportional) error models among others, whereas covariance between the model parameters was ascertained by investigating the unstructured Ω matrix; however, it was only incorporated in the model parameters if the correlations had an absolute value greater than 0.5 (Ette and Williams, 2007).

Even though, the C-t data of this analysis come from a BE study, which implies a relatively homogeneous population, the role of potential covariates was investigated. In this context, several covariates were tested as presented in our previous work (Soulele and Karalis, 2018). In regard to the continuous covariates both linear and allometric relationships were tested, using 70 kg as the standard body weight and fixed exponents: 1 for the volume of distribution and 0.75 for clearance. Correlation between a covariate and EZE (or EZEG) PK parameters were investigated using a backward elimination process. Covariates identified as influential were further assessed for their significance using several methodologies like: stepwise addition, the likelihood ratio test (at $\alpha = 0.05$), the obtained parameter precision, reductions in their percent between-subject variability (BSV%) value, and finally the physiological soundness of its effect on each PK parameter.

The developed PK models were evaluated and compared based on numerical and graphical criteria in addition to the physiological relevance of the estimated PK parameters. The -2 log likelihood, Akaike and Bayesian information criteria were used as numerical selection criteria for the final model selection. Model performance was assessed using the following goodness-of-fit plots: observed versus individual predicted values, individual weighted residuals or normalized prediction distribution errors versus the predicted concentrations, and visual predictive check plots. The latter were used as a diagnostic tool to assess the predictive ability of each model, using the 95% confidence intervals around the 10th, 50th and 90th prediction percentiles from 500 simulated datasets.

3. Results

In total 28 subjects, in the two study periods, were included in the population PK analysis, providing 56 C-t profiles for each drug. It should be clarified that from the initial pool of 36 subjects participating in the BE study, 5 subjects were considered as drop outs from the BE study according to the predefined exclusion criteria and thus no drug C-t data were available for them. In addition, 3 subjects were excluded from this population PK analysis for the following reasons: One of them exhibited rather strange C-t profile where the second concentration peak was much more pronounced than the initial peak. Two other subjects appeared with very high concentration values which led to Cmax estimates three times higher than the average performance. A sensitivity analysis was performed to investigate the influential character of these three subjects on the population PK results. Indeed, when the final model (the one developed without these 3 subjects) was applied to the total dataset, large differences (more than 20%) were observed in many parameters which were as high as 57%. Accordingly, similar high discrepancies were also observed in the % BSV values. Also, when these 3 subjects were included in the dataset, parameter identifiability problems appeared which were reflected on the high conditional number (i.e., 426). In addition, an outlier detection analysis on the individual Cmax, AUCt, and AUCinf values was performed in two ways: a) using a univariate approach based on the inter-quartile range of the data and b) identifying the observations outside the 99th percentile of the normalized Z and t scores of the data. Indeed, both methods recognized the two subjects with very high concentration values as outliers. Therefore, these three subjects were excluded from the population PK analysis in order to get reliable estimates.

The spaghetti plots for EZE and EZEG, displayed in Fig. 1A and B, respectively, reveal the increased complexity and variability of the analyzed datasets. As can be also seen in the average concentration-time profiles of each drug (Fig. 2A and B), the presence of secondary peaks at approximately 5, 12, and 22 h post-dose is consistent with the known enterohepatic recirculation of the EZE and EZEG. As this characteristic was evident in all subjects, an EHC component was incorporated a priori during model construction.

Following a thorough model investigation, and testing of different assumptions regarding the EHC processes, the final model structure for EZE and its active glucuronide, EZEG, is depicted in Fig. 3. The latter is expressed by a model incorporating a pre-systemic transformation of the parent drug into its metabolite which is further coupled with an EHC redistribution loop mimicking the gallbladder physiological action. Key features of this joint population model are the following: a) pre-systemic metabolism of ezetimibe and conversion to its glucuronide metabolite, b) two-compartmental disposition for both EZE and EZEG, and c) inclusion of an EHC component which accounted for the secondary peaks present in both compounds.

In other words, an amount of drug can enter EZE's central compartment with absorption rate 'kap' and at the same time can also arrive at EZEG's central compartment with rate 'kam'. Then, the EZE can either be eliminated from the system with a clearance rate constant 'kelp',

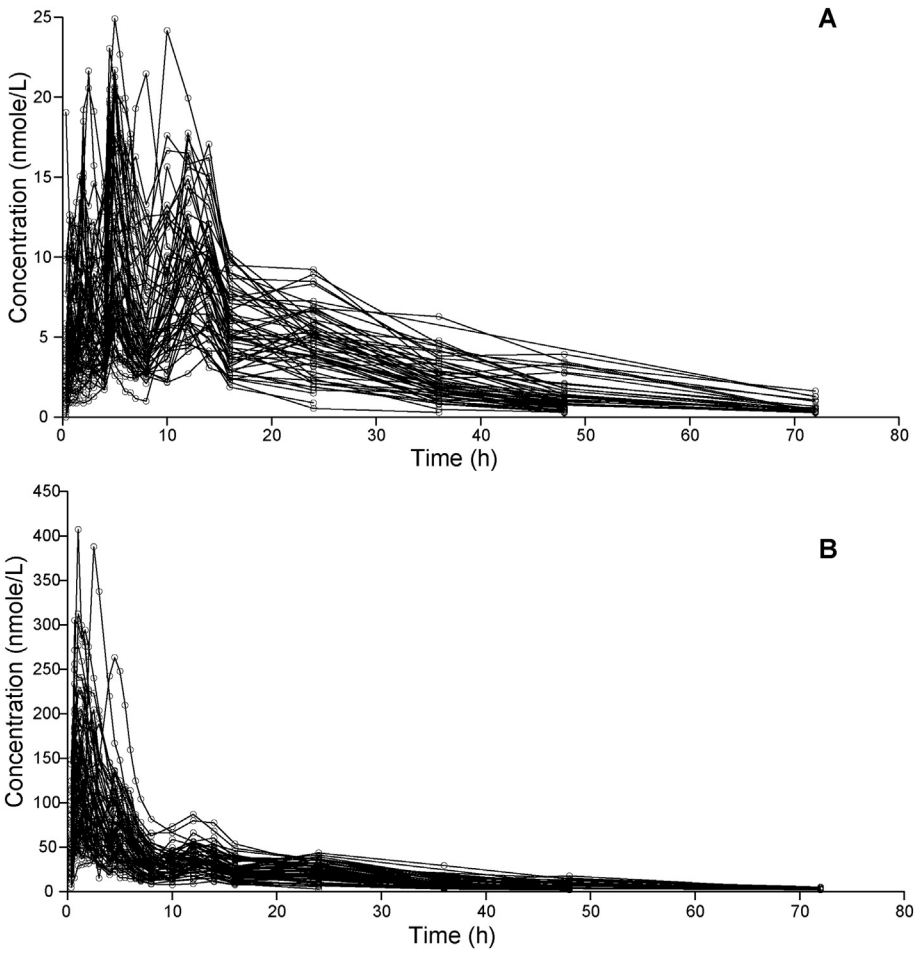

Fig. 1. Spaghetti plots of ezetimibe (A) and ezetimibe-glucuronide (B).

distributed to the peripheral compartment, or be transformed into EZEG by a first-order process. Accordingly, EZEG can either be cleared from the system via a first order process with constant 'kelm', distributed to its peripheral compartment or transferred to the gallbladder compartment. The latter empties at certain time points into the central compartments of both EZE and EZEG. Biliary secretion is modeled by a first-order process and further controlled by a switch on/off function able to mimic intermittent GB emptying. Based on mass balance principle, the corresponding set of ordinary differential equations describes the final best PK model (Fig. 3):

$$dA_{GI}/dt = -kap \cdot A_{GI} - kam \cdot A_{GI} \quad (1)$$

$$dA_{CP}/dt = kap \cdot A_{GI} - (k_{25} + kpm + kelp) \cdot A_{CP} + k_{52} \cdot A_{PP} + GBE \cdot kg_1 \cdot A_{GB} \quad (2)$$

$$dA_{CM}/dt = kam \cdot A_{GI} - (k_{36} + kmb + kelm) \cdot A_{CM} + k_{63} \cdot A_{PM} + kpm \cdot A_{CP} + GBE \cdot kg_2 \cdot A_{GB} \quad (3)$$

$$dA_{GB}/dt = kmb \cdot A_{CM} - GBE \cdot A_{GB} \cdot (kg_1 + kg_2) \quad (4)$$

$$dA_{PP}/dt = k_{25} \cdot A_{CP} - k_{52} \cdot A_{PP} \quad (5)$$

$$dA_{PM}/dt = k_{36} \cdot ACM - k_{63} \cdot A_{PM} \quad (6)$$

$$k_{25} = Qp/Vcp \quad (7)$$

$$k_{52} = Qp/Vpp \quad (8)$$

$$k_{36} = Qm/Vcm \quad (9)$$

$$k_{63} = Qm/Vpm \quad (10)$$

where, *Az* accounts for the amount of drug in the *z* compartment: (GI) the gastrointestinal tract compartment; (CP) the central compartment of EZE; (CM) the central compartment of EZEG; (GB) the gallbladder compartment; (PP) the peripheral compartment of EZE; (PM) the peripheral compartment of EZEG. The term k_{ij} refers to the transfer rate constants among the *i* and *j* compartments, as well as the absorption and elimination constants. The term GBE is a binary factor taking the 0 or 1 values, where GBE equal to 0 simulates the absence of GB emptying and GBE equal to 1 when GB emptying occurs (GBE = 1). Initial conditions for all the compartments were set to zero with the exception of gastrointestinal compartment (A_{GI}), where the entire EZE dose becomes available at zero time.

Three bile release periods (at 4, 11, and 21 h post-dose) were considered for EZEG, whereas the low plasma levels of EZE after 20 h post-dose allowed for the inclusion of only the first two cycles (e.g., 4 and 11 h post-dose). The duration of bile release in each enterohepatic cycle was assumed to be 0.75 h, which approximates the mean duration of gallbladder emptying time in healthy subjects (Berg et al., 2013). Finally, a single PK parameter was used to describe the elimination of each compound, which took place in their central compartments and accounted for both renal and fecal excretion processes. The population PK estimates of the joint PK model of EZE and EZEG, along with their BSV% and percent relative standard errors (RSE%) values are summarized in Table 1.

Between-subject variability for the majority of estimated parameters exhibited moderate values whereas, the relatively low RSE% values obtained for all estimates, indicated that PK parameters could be precisely estimated, suggesting a satisfactory model fitting. A substantial correlation of the random effects between kam-Vcm/F (corr = 0.36)

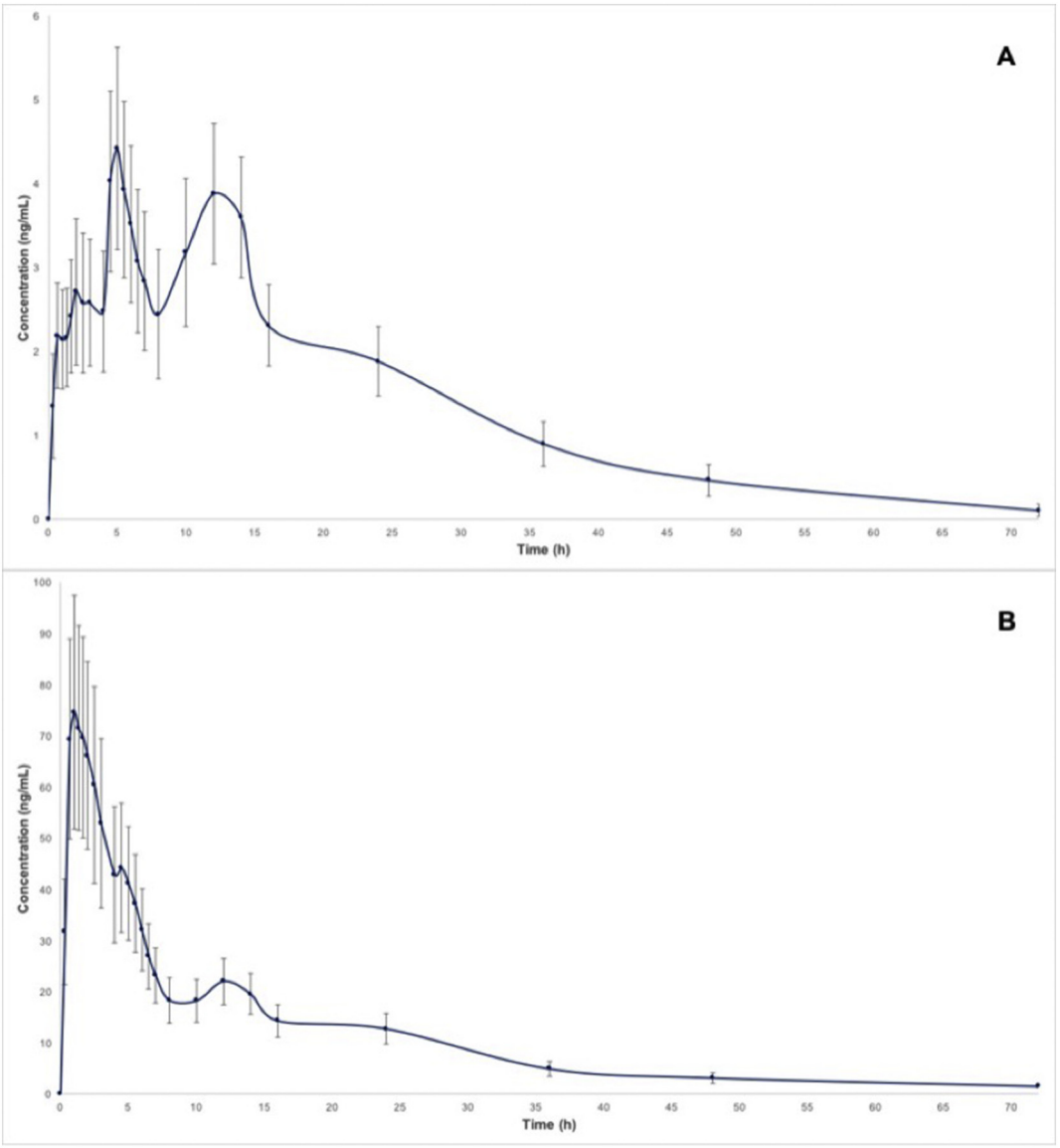

Fig. 2. Mean and individual C-t profiles of ezetimibe (A) and ezetimibe-glucuronide (B) in plasma following a 10 mg single-dose oral administration. Error bars refer to the half of standard deviation.

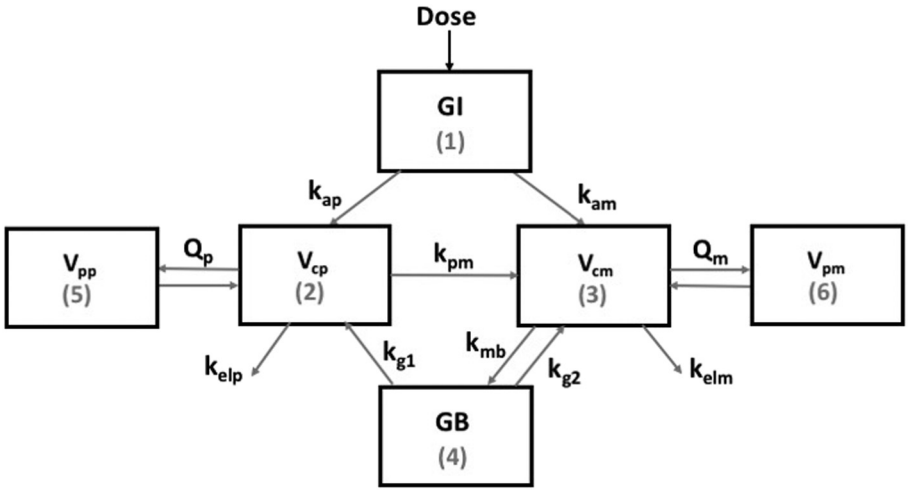

Fig. 3. Schematic representation of the final joint population PK model for ezetimibe (EZE) and ezetimibe-glucuronide (EZEG). *Compartments*: GI, gastrointestinal tract (1); EZE central compartment (2); EZEG central compartment (3); GB, gallbladder (4); EZE peripheral compartment (5); EZEG peripheral compartment (6).

Table 1
Pharmacokinetic parameters for the joint population PK model of EZE and EZEG. *Key*: *b1* and *b2* = residual error parameters for the proportional error model (Eq. (11)).

	Mean (RSE%)	BSV% (RSE%)
PK parameter		
kap (h^{-1})	0.19 (12)	66.88 (14)
kam (h^{-1})	0.49 (8)	43.13 (15)
Vcp/F (L)	223 (5)	22.06 (19)
Vpp/F (L)	698 (8)	42.22 (15)
Qp/F (L/h)	957 (14)	80.09 (15)
kpm (h^{-1})	0.19 (6)	15.69 (31)
kelp (h^{-1})	0.033 (18)	39.64 (44)
kg1 (h^{-1})	1.44 (10)	53.66 (15)
Vcm/F (L)	43.4 (8)	35.99 (16)
Vpm/F (L)	118 (15)	84.79 (15)
Qm/F (L/h)	19.4 (19)	118.76 (15)
kmb (h^{-1})	0.24 (10)	44.95 (19)
kg2 (h^{-1})	0.49 (7)	16.31 (41)
kelm (h^{-1})	0.27 (9)	40.76 (17)
PK random effects correlation		
kam - Vcm/F	0.36 (52)	–
Vpm/F - Qm/F	0.89 (6)	–
Residual error model		
b1	0.37 (2)	–
b2	0.30 (2)	–

and Vpm/F-Qm/F (corr = 0.89) was observed and also included in the final model, providing a significant improvement of the goodness-of-fit criteria.

Residual error for both EZE and EZEG was best described by a proportional error model with a multiplicative coefficient b, according to Eq. (11):

$$C_{ij} = f_{ij} + b \cdot f_{ij} \cdot \varepsilon_{ij} \quad (11)$$

where C_{ij} refers to the observed concentration of EZE of EZEG for the i_{th} individual, b is the parameter of the proportional error model, f_{ij} is the j_{th} model predicted value for i_{th} subject, and ε_{ij} is the random error, assumed to be normally distributed with mean 0 and variance 1. The values of residual error parameters for EZE and EZEG are shown in Table 1. Finally, no covariate effect including demographic characteristics and biochemical values or the treatment and period effects tested, was found to significantly affect the estimated PK parameters, which is in accordance with previous findings on EZE pharmacokinetics (Lipka, 2003).

The main goodness-of-fit plots of the final model for the two agents are presented in Figs. 4–7. Fig. 4 depicts the individual predicted EZE and EZEG concentrations vs. their observed concentration values for the final population PK model. For both EZE and EZEG, an adequate degree of linearity can be observed between the model predicted and observed concentrations.

The balanced distribution around the zero line observed in the individual weighted residuals and normalized prediction distribution errors vs. the individual predicted concentration plots presented in Figs. 5 and 6, respectively, also suggests that the proportional error model chosen in the final model provided an adequate description of the residual unexplained variability of both drugs. Both the individual weighted residuals and normalized prediction distribution errors appear to be randomly distributed around 0 and to be within the required boundaries.

Finally, Fig. 7 displays the visual predictive check plots obtained from the final model for each compound. The predicted values, from the final PK model, were found to describe adequately the observed median and higher concentration values of the two active agents. However, the model was shown to be slightly inferior in regards to the lower concentration values, with a slight underprediction of the second enterohepatic cycle at around 10–13 h post-dose for both drugs, which may be partly attributed to some atypical individual profiles, driving the lower observed percentile estimates.

4. Discussion

Ezetimibe exhibits a complex PK profile greatly influenced by its extensive enterohepatic recirculation. EZE is converted to EZEG, which can be back-transformed to EZE through a repeated re-distribution and de-conjugation process (Kosoglou et al., 2005). Conventional PK compartmental models fail to describe this complex behavior and for such compounds, more sophisticated PK models are required in order to incorporate the complicated metabolism and elimination processes and describe the underlying enterohepatic recirculation process. Other population PK models for EZE found in the literature describe only the PKs of EZE using total ezetimibe concentrations (Ezzet et al., 2001b; Soulele and Karalis, 2018). This study extends our previous work by introducing a joint population PK model for EZE and EZEG. The structure of the current model is quite different from the one developed for total ezetimibe since it takes into consideration the kinetics of both moieties, includes pre-systemic metabolism of EZE and conversion to EZEG, and to the best of our knowledge, this is one of the few joint population PK models for drugs undergoing enterohepatic recirculation. In this respect, a series of structural models were constructed, implementing diverse approaches regarding the metabolism and disposition processes of EZE and EZEG. The first type of models evaluated, did not include first-pass metabolism in the gut and failed to describe the PKs of both drugs (data not shown). The inclusion of a first-pass effect within the gut aid in the description of the early concentration peak observed in EZEG's PK profile. A similar methodology has been previously applied by Bertrand et al. (2011), where they also added first-pass effect in their model allowing to fit adequately the EZEG concentrations. For this reason, first-pass metabolism was intrinsically incorporated in our structural model and the further development focused mainly on the different approaches describing the EHC of the two drugs.

At first, a loop of four compartments was incorporated in the model for the description of EHC, which included the GI tract, the two central compartments, and a theoretical gallbladder compartment, which was designed to deliver drug to the GI tract (from where the two compounds were then re-absorbed back to their central compartments). However, even though pharmacokinetics of EZEG could be adequately described, these types of models were unable to capture the steep concentration fluctuations of EZE. Thus, other approaches were utilized, including one or more theoretical GB compartments, different bile release kinetics, and back-transformation processes. Finally, an adequate description of the EHC process of both drugs was accomplished through the incorporation of one theoretical GB compartment, which was assumed to release both drugs directly to their central compartments by first-order kinetics (Fig. 3). Therefore, a model with first-pass metabolism and an EHC component mimicking the intermittent bile emptying through the gallbladder was developed.

The inclusion of additional compartments such as a theoretical liver compartment, or more PK parameters in the model, e.g. rate constants accounting for fecal elimination, or parameters accounting for the fraction of drug undergoing first-pass metabolism, or enterohepatic recirculation, were also tested for their inclusion in the model, but did not improved model fitting and in many cases led to model overparameterization and poor algorithm convergence.

It is well recognized that such joint multi-compartmental models can have increased complexity and may present parameter identifiability issues and estimation difficulties (Evans et al., 2001; Saccomani and Thomaseth, 2018). In our analysis, to prevent from this possibility certain assumptions were made: i) first-pass effect in the GI tract and subsequent liver metabolism led to the formation of EZEG, ii) all other minor metabolic pathways were disregarded, since the major metabolic pathway of EZE is the phenyl-glucuronidation to EZEG, iii) liver was assumed to be part of the central compartment of EZE, contributing also

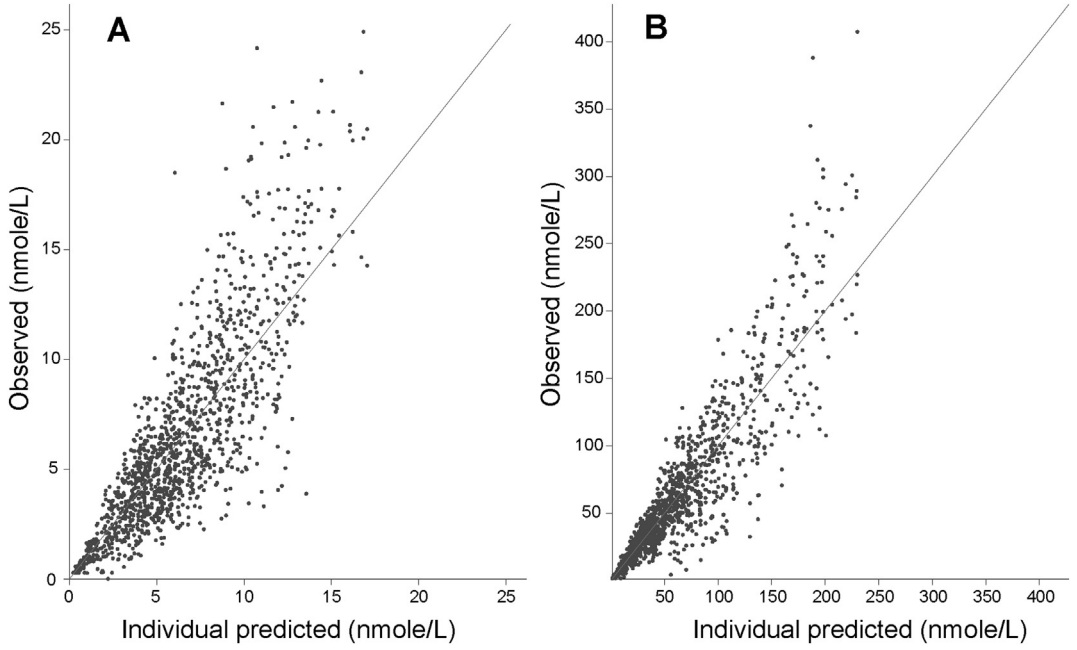

Fig. 4. Observed plasma concentrations versus the individual predicted concentration values of EZE (A) and EZEG (B). The diagonal line represents the line of unity, i.e., the optimal fitting.

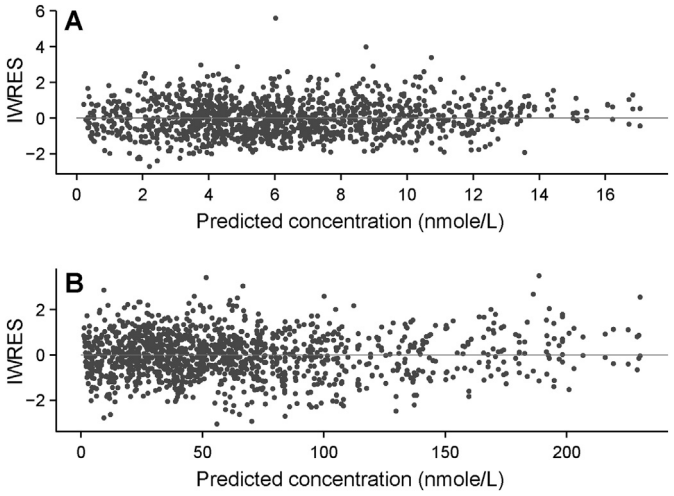

Fig. 5. Plot of the individual weighted residuals (IWRES) versus the individual predicted concentrations of EZE (A) and EZEG (B) for the final model. The horizontal line represents the zero line, namely, the ideal situation.

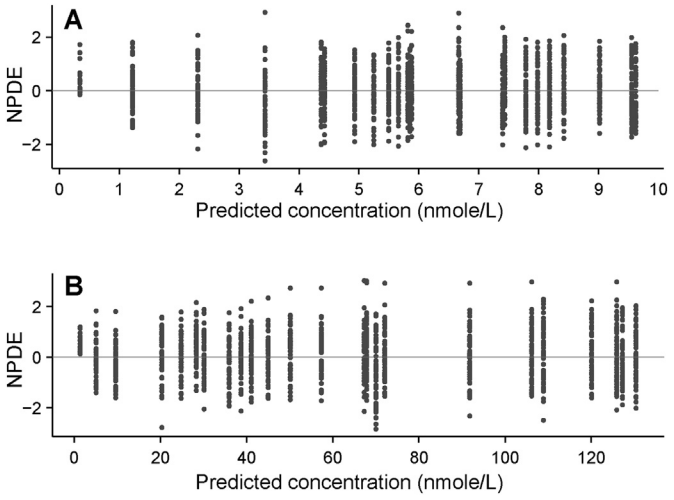

Fig. 6. Normalized prediction distribution errors (NPDE) versus the individual predicted concentrations of EZE (A) and EZEG (B) for the final model. The horizontal line represents the ideal situation, i.e. the zero line.

to the direct transformation of EZE into EZEG, iv) gallbladder emptying time and duration were fixed to certain values, based on information regarding gallbladder physiology and the study protocol, v) three enterohepatic cycles were considered for EZEG (i.e., at 4, 11, and 21 h), whereas in the case of EZE the very low plasma levels of the drug allowed the inclusion of only the first two cycles (i.e., at 4 and 11 h), vi) drugs excreted from the GB were hypothesized to be delivered directly back to the central compartments of the drugs, accounting also for the glucuronide conjugate hydrolysis and finally vii) a universal rate constant was considered to describe both fecal and renal elimination which followed first-order kinetics and took place in the central compartment of each drug. It should be mentioned that setting fixed the gallbladder emptying times is an already established technique in population PK modeling (Jiao et al., 2008; Sam et al., 2009; Sherwin et al., 2012). The appropriately selected final model, along with the abovementioned assumptions, led to a model where PK parameters could be identified nicely. Indeed, the conditional number was 12 (the minimum and maximum eigenvalue of the Fisher information matrix were 0.16 and 1.9, respectively), the % relative standard error values were relatively low (Table 1), and the convergence assessment led to favorable findings where the % coefficient of variation for all parameters after 5 runs, with randomly generated initial values for all parameters and different seeds, ranged from 7% to 18%.

The final model was able to adequately fit to the observed C-t data of both EZE and EZEG and provided rational PK estimates. Population mean estimates obtained for the final model for EZE and EZEG (Table 1) were found to be physiologically relevant and approximated previously published values (Ezzet et al., 2001b; Jeu and Cheng, 2003; Soulele and Karalis, 2018). The relatively high apparent volumes of distribution and low clearance values were consistent with the extensive enterohepatic recycling (Colburn, 1982; Roberts et al., 2002; Smith et al., 2015).

No significant covariate effect was found on any of the estimated PK parameters. The inclusion of a relatively small number of subjects, derived from a relatively homogenous healthy population (which is

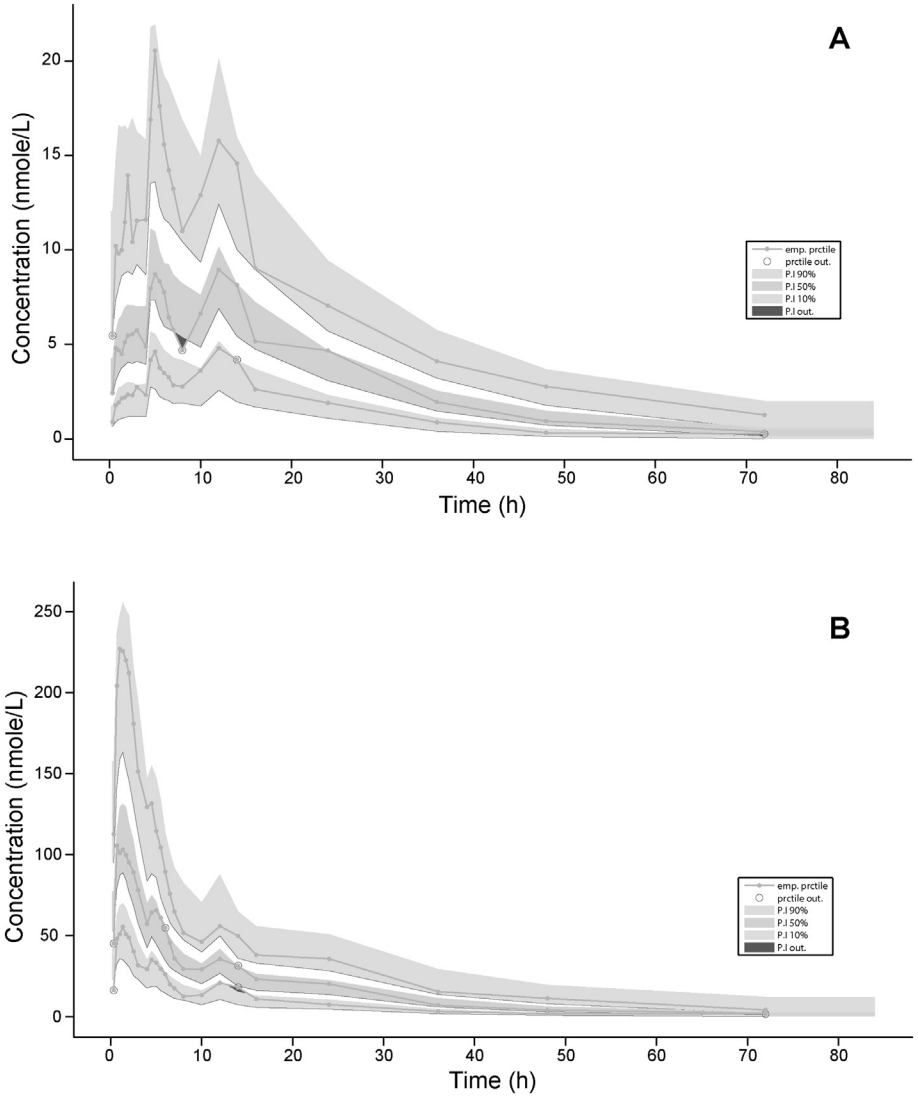

Fig. 7. Visual predictive check plots of the final PK model for EZE (A) and EZEG (B). *Key*: Solid lines represent the 10th, 50th, and 90th percentiles of the observed data; Shaded areas represent the 95% prediction intervals around each theoretical percentile; circles and dark shaded areas denote the outlier data.

typically enrolled in BE studies), as well as the increased model complexity, may also account for the absence of a significant covariate effect in this analysis. In any case, EZE pharmacokinetics has been shown not to be significantly influenced by age, gender, race or the presence of renal or hepatic abnormalities in previous studies (Jeu and Cheng, 2003; Kosoglou et al., 2005).

Overall, the most striking aspect of this analysis was the development of a joint population PK model for ezetimibe that could sufficiently describe the complex pharmacokinetics of EZE and EZEG simultaneously. This model, although considering the physiological complexity of enterohepatic recirculation, is parsimonious because it incorporates the underlying processes of conjugate hydrolysis and reabsorption in one step, facilitating model fitting and PK parameters estimation. Extension of this EHC model to other population groups, including patients with hypercholesterolemia, those of different age or ethnicity or patients receiving concomitant medication, would provide further insight on ezetimibe kinetics.

5. Conclusions

In the present study, a joint population PK model was developed for ezetimibe and ezetimibe-glucuronide, which could adequately describe the complex pharmacokinetics of both moieties in healthy individuals. The inclusion of first-pass effect within the gut allowed to capture the early concentration peak seen in EZEG's concentration-time profile. Enterohepatic recirculation was modeled through the incorporation of a theoretical gallbladder compartment which allowed the description of subsequent concentration peaks. Population estimates obtained for the final model for EZE and EZEG were physiologically relevant, while the relatively high apparent volumes of distribution and low clearance values were consistent with the extensive enterohepatic recycling. No significant covariate effect was found on any of the estimated PK parameters in line with previously published studies.

Declarations of interest

None.

Acknowledgements

The authors would like to thank Rafarm S.A. Athens, Greece for providing the data for this analysis. We would also like to thank Ms. Eleni Rerra for her contribution to part of the computational work.

Funding

This research did not receive any specific grant from funding agencies in the public, commercial, or not-for-profit sectors.

References

Berg, A.K., Mandrekar, S.J., Ziegler, K.L., Carlson, E.C., Szabo, E., Ames, M.M., ... Reid, J.M., 2013. Population pharmacokinetic model for cancer chemoprevention with sulindac in healthy subjects. J. Clin. Pharmacol. 53 (4), 403–412.

Bertrand, J., Laffont, C.M., Mentré, F., Chenel, M., Comets, E., 2011. Development of a complex parent-metabolite joint population pharmacokinetic model. AAPS J. 13 (3), 390–404.

Colburn, W.A., 1982. Pharmacokinetic and biopharmaceutic parameters during enterohepatic circulation of drugs. J. Pharm. Sci. 71 (1), 131–133.

de Waart, D.R., Vlaming, M.L., Kunne, C., Schinkel, A.H., Oude Elferink, R.P., 2009. Complex pharmacokinetic behavior of ezetimibe depends on abcc2, abcc3, and abcg2. Drug Metab. Dispos. 37 (8), 1698–1702. https://doi.org/10.1124/dmd.108.026146.

Ette, E.I., Williams, P.J., 2007. Pharmacometrics: The Science of Quantitative Pharmacology. John Wiley and Sons, Inc., Hoboken, NJ.

Evans, N.D., Godfrey, K.R., Chapman, M.J., Chappell, M.J., Aarons, L., Duffull, S.B., 2001. An identifiability analysis of a parent–metabolite pharmacokinetic model for ivabradine. J. Pharmacokinet. Pharmacodyn. 28, 93. https://doi.org/10.1023/A:1011521819898.

Ezzet, F., Wexler, D., Statkevich, P., Kosoglou, T., Patrick, J., Lipka, L., Mellars, L., Veltri, E., Batra, V., 2001a. The plasma concentration and LDL-C relationship in patients receiving ezetimibe. J. Clin. Pharmacol. 41 (9), 943–949.

Ezzet, F., Krishna, G., Wexler, D.B., Statkevich, P., Kosoglou, T., Batra, V.K., 2001b. A population pharmacokinetic model that describes multiple peaks due to enterohepatic recirculation of ezetimibe. Clin. Ther. 23 (6), 871–885.

Florentin, M., Liberopoulos, E.N., Elisaf, M.S., 2008. Ezetimibe-associated adverse effects: what the clinician needs to know. Int. J. Clin. Pract. 62 (1), 88–96. https://doi.org/10.1111/j.1742-1241.2007.01592.x.

Ghosal, A., Hapangama, N., Yuan, Y., Achanfuo-Yeboah, J., Iannucci, R., Chowdhury, S., Alton, K., Patrick, J.E., Zbaida, S., 2004. Identification of human UDP-glucuronosyltransferase enzyme(s) responsible for the glucuronidation of ezetimibe (Zentia). Drug Metab. Dispos. 32 (3), 314–320.

Hajar, R., 2017. Risk factors for coronary artery disease: historical perspectives. Heart Views 18 (3), 109–114. https://doi.org/10.4103/HEARTVIEWS.HEARTVIEWS_106_17.

Jeu, L., Cheng, J.W., 2003. Pharmacology and therapeutics of ezetimibe (SCH 58235), a cholesterol-absorption inhibitor. Clin. Ther. 25 (9), 2352–2387.

Jiao, Z., Ding, J.J., Shen, J., Liang, H.Q., Zhong, L.J., Wang, Y., Zhong, M.K., Lu, W.Y., 2008. Population pharmacokinetic modelling for enterohepatic circulation of mycophenolic acid in healthy Chinese and the influence of polymorphisms in UGT1A9. Br. J. Clin. Pharmacol. 65 (6), 893–907.

Klag, M., Ford, D.E., Mead, L.A., He, J., Whelton, P.J., Liang, K.-Y., Levine, D.M., 1993. Serum cholesterol in young men and subsequent cardiovascular disease. N. Engl. J. Med. 328, 313–318.

Kosoglou, T., Statkevich, P., Fruchart, J.C., Pember, L.J., Reyderman, L., Cutler, D.L., Guillaume, M., Maxwell, S.E., Veltri, E.P., 2004. Pharmacodynamic and pharmacokinetic interaction between fenofibrate and ezetimibe. Curr. Med. Res. Opin. 20 (8), 1197–1207.

Kosoglou, T., Statkevich, P., Johnson-Levonas, A.O., Paolini, J.F., Bergman, A.J., Alton, K.B., 2005. Ezetimibe: a review of its metabolism, pharmacokinetics and drug interactions. Clin. Pharmacokinet. 44 (5), 467–494.

Lipka, L.J., 2003. Ezetimibe: a first-in-class, novel cholesterol absorption inhibitor. Cardiovasc. Drug Rev. 21 (4), 293–312.

Patrick, J.E., Kosoglou, T., Stauber, K.L., Alton, K.B., Maxwell, S.E., Zhu, Y., ... Cayen, M.N., 2002. Disposition of the selective cholesterol absorption inhibitor ezetimibe in healthy male subjects. Drug Metab. Dispos. 30 (4), 430–437.

Roberts, M.S., Magnusson, B.M., Burczynski, F.J., Weiss, M., 2002. Enterohepatic circulation: physiological, pharmacokinetic and clinical implications. Clin. Pharmacokinet. 41 (10), 751–790.

Saccomani, M.P., Thomaseth, K., 2018. The union between structural and practical identifiability makes strength in reducing oncological model complexity: a case study. Complexity, 2380650. https://doi.org/10.1155/2018/2380650. (Hindawi, 10 pages).

Sam, W.J., Akhlaghi, F., Rosenbaum, S.E., 2009. Population pharmacokinetics of mycophenolic acid and its 2 glucuronidated metabolites in kidney transplant recipients. J. Clin. Pharmacol. 49 (2), 185–195.

Sherwin, C.M., Sagcal-Gironella, A.C., Fukuda, T., Brunner, H.I., Vinks, A.A., 2012. Development of population PK model with enterohepatic circulation for mycophenolic acid in patients with childhood-onset systemic lupus erythematosus. Br. J. Clin. Pharmacol. 73 (5), 727–740.

Smith, D.A., Beaumont, K., Maurer, T.S., Di, L., 2015. Volume of distribution in drug design. J. Med. Chem. 58 (15), 5691–5698.

Soulele, K., Karalis, V., 2018. On the population pharmacokinetics and the enterohepatic recirculation of total ezetimibe. Xenobiotica 27, 1–11. https://doi.org/10.1080/00498254.2018.1463117.

Sweeney, M.E., Johnson, R.R., 2007. Ezetimibe: an update on the mechanism of action, pharmacokinetics and recent clinical trials. Expert Opin. Drug Metab. Toxicol. 3 (3), 441–450. https://doi.org/10.1517/17425255.3.3.441.

van Heek, M., Davis, H., 2002. Pharmacology of ezetimibe. Eur. Heart J. Suppl. 4 (Suppl. J), J5–J8.